J Physiol 592.24 (2014) pp 5409–5427

The Journal of Physiology

Distinct roles of L- and T-type voltage-dependent Ca^{2+} channels in regulation of lymphatic vessel contractile activity

Stewart Lee, Simon Roizes and Pierre-Yves von der Weid

Inflammation Research Network and Smooth Muscle Research Group, Snyder Institute for Chronic Diseases, Department of Physiology & Pharmacology, Cumming School of Medicine, University of Calgary, Calgary, Alberta, Canada

Key points

- Lymph transport is promoted by lymphatic pumping, a robust phasic contractile activity of the collecting lymphatic vessels. This contractile function, critical for tissue fluid homeostasis and immune cell transport to lymph nodes, is regulated by the amount of lymph entering the vessels and subsequent distension of the vessel wall.
- While lymphatic pumping relies on influx of Ca^{2+} through voltage-dependent Ca^{2+} channels, characterization of these channels and details of their contribution to the regulation of stretch-activated contractions are lacking.
- Here we report the expression of L- and T-type Ca^{2+} channels in rat mesenteric lymphatic vessels and their differential role in regulating strength and frequency of lymphatic contractions.
- This study fosters our knowledge on the mechanisms that drive stretch-activated lymphatic contractions. It may help in providing a basis to developing agents able to enhance lymphatic function, which could be of therapeutic benefit during lymphatic impairment such as lymphoedema.

Abstract Lymph drainage maintains tissue fluid homeostasis and facilitates immune response. It is promoted by phasic contractions of collecting lymphatic vessels through which lymph is propelled back into the blood circulation. This rhythmic contractile activity (i.e. lymphatic pumping) increases in rate with increase in luminal pressure and relies on activation of nifedipine-sensitive voltage-dependent Ca^{2+} channels (VDCCs). Despite their importance, these channels have not been characterized in lymphatic vessels. We used pressure- and wire-myography as well as intracellular microelectrode electrophysiology to characterize the pharmacological and electrophysiological properties of L-type and T-type VDCCs in rat mesenteric lymphatic vessels and evaluated their particular role in the regulation of lymphatic pumping by stretch. We complemented our study with PCR and confocal immunofluorescence imaging to investigate the expression and localization of these channels in lymphatic vessels. Our data suggest a delineating role of VDCCs in stretch-induced lymphatic vessel contractions, as the stretch-induced increase in force of lymphatic vessel contractions was significantly attenuated in the presence of L-type VDCC blockers nifedipine and diltiazem, while the stretch-induced increase in contraction frequency was significantly decreased by the T-type VDCC blockers mibefradil and nickel. The latter effect was correlated with a hyperpolarization. We propose that activation of T-type VDCCs depolarizes membrane potential, regulating the frequency of lymphatic contractions via opening of L-type VDCCs, which drive the strength of contractions.

DOI: 10.1113/jphysiol.2014.280347

(Received 2 July 2014; accepted after revision 29 September 2014; first published online 17 October 2014)
Corresponding author P.-Y. von der Weid: Department of Physiology & Pharmacology, Cumming School of Medicine, University of Calgary, 3330 Hospital Drive N.W., Calgary, Alberta, Canada T2N 4N1. Email: vonderwe@ucalgary.ca

Abbreviations AP, action potential; APSS, physiological saline solution with albumin; DAPI, 4′,6-diamidino-2-phenylindole; DPBS, Dulbecco's phosphate-buffered saline; STD, spontaneous transient depolarization; VDCC, voltage-dependent Ca^{2+} channels; V_m, membrane potential.

Introduction

The principal function of the lymphatic system in mammals, including humans, is to transport lymph throughout the body from peripheral tissues to the great veins of the neck (Zawieja, 2009). This function is important for tissue fluid homeostasis as it allows excess interstitial fluid to be returned to the blood stream, but is also critical to immune surveillance and fat distribution, as lymph containing most digested long-chain fatty acids and immune cells is transported to and from lymph nodes. This lymph transport is mainly achieved by the intrinsic ability of the lymphatic muscle cells in the wall of collecting lymphatic vessels to contract rhythmically, causing transient compression of chambers (also known as lymphangions) that comprise the vessels. Contractions of the lymphangions, which are close-ended by valves, propel lymph in a one-way direction in a pulsatile manner described as lymphatic pumping. Importantly, lymphatic vessel contractions are sensitive to a physical stimulus, such as distension of the vessel wall, as occurs during elevated luminal pressure. This mechanism, called 'stretch activation', leads to an increase in frequency and amplitude of contractions (McHale & Roddie, 1976; Hargens & Zweifach, 1977; Gashev *et al.* 2004). Furthermore, these contractions are initiated in the lymphatic muscle by a pacemaker-generated action potential (AP) (Azuma *et al.* 1977; Kirkpatrick & McHale, 1977; Allen *et al.* 1983). Earlier studies using intracellular microelectrode recordings on guinea pig mesenteric lymphatic vessels showed that the pacemaking mechanism relies on spontaneous transient depolarizations (STDs), events demonstrated to reflect the synchronized release of Ca^{2+} through inositol triphosphate (IP_3) receptors in the sarcoplasmic reticulum, and causing the opening of Ca^{2+}-activated chloride channels (Van Helden, 1993; von der Weid *et al.* 2008). Spatial and temporal summation of STDs leads to AP generation, consequent to opening of voltage-dependent Ca^{2+} channels (VDCCs), allowing entry of extracellular Ca^{2+}, and vessel contraction (van Helden *et al.* 1995; Imtiaz *et al.* 2007).

The VDCCs are a superfamily of pore-forming genes consisting of 10 members, classified into subfamilies according to their α-subunit composition (Hofmann *et al.* 1999; Lacinova, 2005). Among them, L-type and T-type Ca^{2+} channels ($Ca_v1.1$–1.4 and $Ca_v3.1$–3.3, respectively) have been primary targets of investigation in many muscle cells; however, characterization of these channels and their involvement in the contractions of lymphatic muscle have been inadequately addressed. What has been demonstrated so far is that APs and subsequently lymphatic contractions are inhibited by dihydropyridines, and are thus deemed to originate from inward Ca^{2+} currents through L-type Ca^{2+} channels (Azuma *et al.* 1977; McHale *et al.* 1987; Atchison & Johnston, 1997; Hollywood *et al.* 1997). L-type, also known as 'long-lasting', Ca^{2+} channels are characterized by their large single channel conductance amplitude, and an activation threshold at a higher membrane voltage of approximately –30 mV (Hirano *et al.* 1989). In a typical smooth muscle cell, depolarization of the membrane potential leads to opening of L-type Ca^{2+} channels and entry of extracellular Ca^{2+} to increase intracellular Ca^{2+} levels and promote contraction. The presence of L-type currents in smooth muscle tissues has been widely demonstrated (Nelson *et al.* 1990; Snutch *et al.* 2001), and shown to play a role in myogenic smooth muscle contractions (Nelson *et al.* 1990; Knot & Nelson, 1995, 1998; Moosmang *et al.* 2003), mechanisms of stretch activation (Langton, 1993; Xu *et al.* 1996; Kimura *et al.* 2000) and membrane potential depolarization (Davis *et al.* 1992; Welsh *et al.* 2000, 2002).

In contrast, T-type Ca^{2+} channels, known as 'transient' Ca^{2+} channels, exhibit a small amplitude of conductance and a low activation threshold at a membrane potential of approximately –70 mV (Hirano *et al.* 1989). The transient action of T-type Ca^{2+} channels has raised questions regarding the extent to which they could contribute to the function of excitable cells, as short time of activation and small inward conductance may mean a lesser amount of extracellular Ca^{2+} ions entering the cell. However, there is still a growing body of evidence of T-type Ca^{2+} channels providing a feasible route for extracellular Ca^{2+} entry (Bradley *et al.* 2004; Kuo *et al.* 2010), and they have been implicated as a possible pacemaker component in the heart and cardiac tissues (Hagiwara *et al.* 1988; Liu *et al.* 1993). T-type Ca^{2+} channels have, however, not yet been identified or characterized in rat mesenteric lymphatic vessels. The present study focuses on the characterization of L-type and T-type VDCCs in lymphatic vessels and their roles in pumping and stretch regulation.

Methods

Ethical approval

Male Sprague Dawley rats (150–250 g, Charles River, QC, Canada) were used to perform all experiments. Animals were allowed full access to food and water; both normal circadian rhythms and body temperatures were maintained. All animal protocols were reviewed and approved by the University of Calgary Animal Care and Ethics Committee and were conducted in accordance with the guidelines of the Canadian Council on Animal Care and the National Institutes of Health's *Guide for the Care and Use of Laboratory Animals*.

Lymphatic vessel preparation

The lymphatic vessels were isolated in two ways to allow investigations under resting and stretched conditions. To investigate lymphatic vessels under stretched conditions, the rats were anaesthetized with ketamine (1 ml kg^{-1}), xylazine (100 μl kg^{-1}) and diazepam (375 μl kg^{-1}). A laparotomy was performed and a loop of small intestine close to the caecum (3–5 cm long) was gently exteriorized on to a specially designed dissection board. The mesentery containing lymphatic and blood vessels, and surrounding fat was then clearly visible. The exposed gut and mesentery were continuously moistened with Dulbecco's phosphate-buffered saline (DPBS; Sigma, St Louis, MO, USA) throughout the procedure. With the help of an inverted stereomicroscope (Leica, Wetzlar, Germany), lymphatic vessels of approximately 2.0 mm in length were identified, gently cleared of connective tissue and fat with fine tweezers, dissected out and transferred to a 35 mm Petri dish containing MOPS-buffered physiological saline solution with albumin (APSS; 145 mM NaCl, 5 mM KCl, 2.5 mM $CaCl_2$, 1 mM $MgSO_4$, 1 mM NaH_2PO_4, 0.02 mM EDTA, 2 mM pyruvate, 5 mM glucose, 3 mM Mops, 0.5% purified bovine albumin). Upon vessel isolation, the animal was killed by decapitation (Davis *et al.* 2007; Dougherty *et al.* 2008).

For lymphatic vessel studies under resting conditions, the rats were killed by decapitation during deep anaesthesia induced by inhalation of isoflurane. The small intestine with its attached mesentery was rapidly dissected and placed in a container filled with APSS. A small ileal piece of mesentery containing collecting lymphatic vessels and their associated artery and vein were dissected, pinned down to a Sylgard-covered small organ bath (100 μl volume) and placed on the stage of an inverted microscope. The section of the mesentery was chosen to contain the most visible lymphatic vessel, and limited amount of fat cells surrounding the vessel. The organ bath was continuously superfused with APSS heated to 36°C at a flow rate of 3 ml min^{-1}. Layer(s) of mesenteric fat were sometimes carefully cleaned to make a small opening (0.5–1 mm) so that the lymphatic vessel could be visualized and accessed. Vessels mounted in such a manner are referred to here as 'unstretched vessels'.

Pressure myography

A segment of the lymphatic vessel was cannulated with two glass pipettes inserted into the lumen of the lymphatic vessel (approximate diameter: 80–120 μm) positioned just above a glass cover slip comprising the bottom of a 2 ml organ bath. Once cannulated, the lymphatic vessel was tied at each end with a fine suture to the glass pipettes, which restricted lymph flow, leakage of lymph as well as pressure drops inside the lymphatic vessel. Each glass pipette was connected to independently adjustable pressure reservoirs (Duling *et al.* 1981). The pressure reservoirs were filled with APSS and positioned at adjustable heights to allow the experimenter to adjust the luminal pressure of the lymphatic vessel. The organ bath was superfused with APSS at a physiologically relevant temperature (37°C) at a rate of 3 ml min^{-1}, and the vessel was exposed for an equilibrium period of 30–60 min to a pressure of 2–3 cmH_2O to establish steady phasic contractions.

After the equilibrium period and steady phasic contractions were observed, a ramp protocol was performed (Fig. 1). The ramp protocol consisted of an increase in luminal pressure from 0 to 12 cmH_2O in steps of 1 cmH_2O. Each step allowed 1 min for equilibration at the luminal pressure, and another minute in which contraction frequency and diameter changes during contractions were measured. A maximum applied pressure of 12 cmH_2O was chosen because both amplitude and contraction frequency plateaued over the range 10–12 cmH_2O. This protocol was repeated twice, once in control conditions and following a 30 min incubation in the presence of a pharmacological blocker. Diameter changes of the lymphatic vessel wall were measured using a video dimension analyser (Model V94; Living Systems Instrumentation, Burlington, VT, USA). The analyser tracks the optically denser lymphatic vessel wall and the measurements are sent to the computer via an analog-to-digital converter (PowerLab/4SP; ADInstruments, Mountain View, CA, USA). Using Chart5 software, the amplitude of contractions was calculated as the difference in diameter between diastolic and systolic phases of the contraction. A decrease in diameter in the shape of a downward spike was counted as a contraction.

Wire myography

Two 25 mm long, 25 μm outer diameter, stainless steel wires were carefully passed, one at a time, through the lumen of a lymphatic vessel segment. The vessel was then

transferred to the organ chamber of a single-channel, wire myograph (Model 310A; Danish Myo Technology, Aarhus, Denmark). The wires were secured to the myograph jaws and minimal force was applied during a 30 min warming step (36–37°C). During the process, DPBS was replaced with warm APSS of the following composition (mM): NaCl 145, KCl 5, $CaCl_2$ 2.5, $MgSO_4$ 1, NaH_2PO_4 1, EDTA 0.02, pyruvate 2, glucose 5, Mops 3, purified BSA 0.5 g 100 ml^{-1}, with pH adjusted to 7.4 at 37°C. Passive force (preload) was then set to 0.2 mN. Spontaneous force transients typically started after 5–10 min, with stable frequency and amplitude occurring over the course of a 60 min equilibration period. As illustrated in Fig. 2, step-increase protocols were applied to vary vessel tension, and spontaneous force transients were recorded (Davis *et al.* 2007) together with lymphatic muscle membrane potential (V_m) (see description below).

Electrophysiology

Impalements of lymphatic muscle were obtained from the adventitial side of the vessels. V_m was recorded under resting conditions (unstretched vessels) and during changes in preload (wire myograph mounted vessels) with conventional glass intracellular microelectrodes filled with 0.5 M KCl (resistance 150–250 MΩ). The microelectrode was connected to an amplifier (Intra 767; World Precision Instruments, Sarasota, FL, USA) through an Ag–AgCl half-cell and recorded on a computer via an analog-to-digital converter (PowerLab/4SP). Lymphatic muscle impalements were characterized by a sharp drop in potential that settled after 10–15 s to −40 to −45 mV in unstretched conditions (von der Weid *et al.* 1996; Fox & von der Weid, 2002). When experiments were performed on vessels mounted on the wire myograph, impalements could only be successfully obtained and maintained when a minimal preload (≥0.1 mN) was applied to the myograph and, as a consequence, the vessel was slightly stretched. Under these conditions, the resting V_m value recorded was usually not more negative than −40 mV (typically between −30 and −35 mV). V_m was corrected at the end of the impalement by subtracting the voltage value obtained after pulling the electrode out of the muscle to that of the measured intracellular value. The underlying causes for the depolarized V_m in myograph-mounted vessels were determined to be due to a combination of stretch and damage to the endothelium caused by the luminal insertion of the stainless steel wires (see von der Weid *et al.* 2014).

Nested PCR

A piece of mesentery from the ileum region containing lymphatic vessels was pinned on a Sylgard-coated organ bath filled with RNA-stabilizing agent RNAlater (Qiagen, Mississauga, ON, Canada). Lymphatic vessels were then isolated from the mesentery. Control tissues such as brain, skeletal muscle and retina were dissected after the animal had been killed. All tissue samples were immediately immersed into RNase- and DNase-free collection tubes containing RNAlater, kept at 4°C overnight and stored at −20°C. Tissues were then homogenized using a QIAshredder (Qiagen) and mRNA was extracted using the Qiagen Micro RNeasy Kit (Qiagen). cDNA was subsequently synthesized using Superscript II Reverse Transcriptase enzyme (Invitrogen, Burlington, ON, Canada) with oligo (dT) primers. Nested PCR was used to improve the sensitivity of detection of products by amplifying the target sequences twice using two sets of primers, one of which is 'nested within' the other set of primers. Target sequences were amplified twice (40 cycles each) with a thermal cycler (Bio-Rad, Mississauga, ON, Canada) using 2× PCR Master Mix (Thermo Scientific, Ottawa, ON, Canada) and two sets of respective primers. Primer sequences were designed with a combination of the Primer3 and Basic Local Alignment Search Tool (Primer-BLAST) software to amplify mRNA sequences of the rat α_1 pore-forming subunit of L-type Ca^{2+} channels ($Ca_v1.1$, 1.2, 1.3 and 1.4) and T-type Ca^{2+} channels ($Ca_v3.1$, 3.2 and 3.3) of rat sequences (see Table 1). The amplified products were loaded into wells in a 2% agarose gel (Invitrogen) set up on a horizontal electrophoresis chamber (Mini-Sub Cell GT system; Bio-Rad) and labelled with 0.2 $\mu g\,ml^{-1}$ ethidium bromide. A pre-stained control ladder (1 Kb Plus DNA ladder; Invitrogen) was used to estimate the base pair size of each product. Control tissues for each respective primer set were used as positive control and negative control experiments were performed in the absence of the forward primer, or absence of cDNA. Fluorescence was detected by trans UV radiation on a ChemiDoc SRS+ system (Bio-Rad).

Immunofluorescence imaging

Segments of lymphatic vessels were isolated as described above in the stretched condition method. The isolated lymphatic vessels were fixed and permeabilized in PBS containing 4% formalin (Sigma) and 0.5% Triton (BDH Inc., Toronto, ON, Canada) for 1 h. The vessels were then washed and blocked with PBS containing 3% goat serum (Sigma), 1% BSA (Sigma) and 0.05% Tween 20 (EMD Millipore Chemicals, Darmstadt, Germany) for 1 h at room temperature and incubated overnight with the respective primary antibodies: α-actin (Sigma), $Ca_v1.2$ and $Ca_v3.2$ (Alomone, Jerusalem, Israel) at dilutions of 1:100 (primary antibody to blocking solution). The vessels were then washed with PBS containing 0.5% Triton and incubated for 1 h in the same buffer solution

containing secondary goat anti-mouse antibody Alexa Fluor 647 (A21241; Invitrogen) and goat antibody Alexa Fluor 488 (A11008; Invitrogen) in concentrations of 1:500 (secondary antibody to buffer solution) for 1 h at room temperature. After wash with DPBS, the vessels were incubated with 4′,6-diamidino-2-phenylindole (DAPI; Invitrogen) at a dilution of 1:500 for nucleus labelling. Vessels were then secured on the glass bottom of a vessel chamber and imaged using an FV1000 confocal microscope (Olympus, Tokyo, Japan). The immunofluorescence was detected and images recorded in z stacks. Positive controls for the vessels contained DAPI for nuclear labelling, α-actin antibody to identify muscle cells and either $Ca_v1.2$ or $Ca_v3.2$ primary antibody for L-type or T-type Ca^{2+} channel labelling, respectively. Two different negative control experiments were performed, first by not including the primary antibody, and second by adding the immunizing peptide provided by Alomone to the primary antibody incubation solution.

Chemicals and materials

The following reagents were used: nickel (II) chloride (Ni^{2+}) and mibefradil from Sigma-Aldrich; and nifedipine and diltiazem from Calbiochem (Billerica, MA, USA). Nifedipine was dissolved in DMSO and Ni^{2+}, mibefradil and diltiazem in distilled water to make 10 mM stock solutions (300 and 100 μM for nifedipine), which were subsequently diluted in APSS to achieve their respective final concentrations. The final concentration of each vehicle was always $\leq 0.1\%$ (v/v), a concentration that had no effect on lymphatic contractile and electrical activities.

Data and statistical analysis

Experimental data are expressed as mean values ± SEM. Statistical significance was assessed using two-tailed paired Student's *t* test, or two-way ANOVA with Bonferroni's *post hoc* test as indicated in the text. A *P* value below 0.05 was considered significant.

Results

Effect of stretch on rat lymphatic vessel contractile activity

The effect of luminal pressure was assessed on cannulated rat mesenteric lymphatic vessels mounted on a pressure myograph. An increase in intraluminal pressure caused an increase in contraction frequency up to a maximum of 15 ± 2 contractions min^{-1} attained at pressures of 8–10 cmH_2O, when a plateau was reached ($n = 4$). The amplitude of contractions initially increased up to 75 ± 8 μm at 4 cmH_2O and then gradually decreased

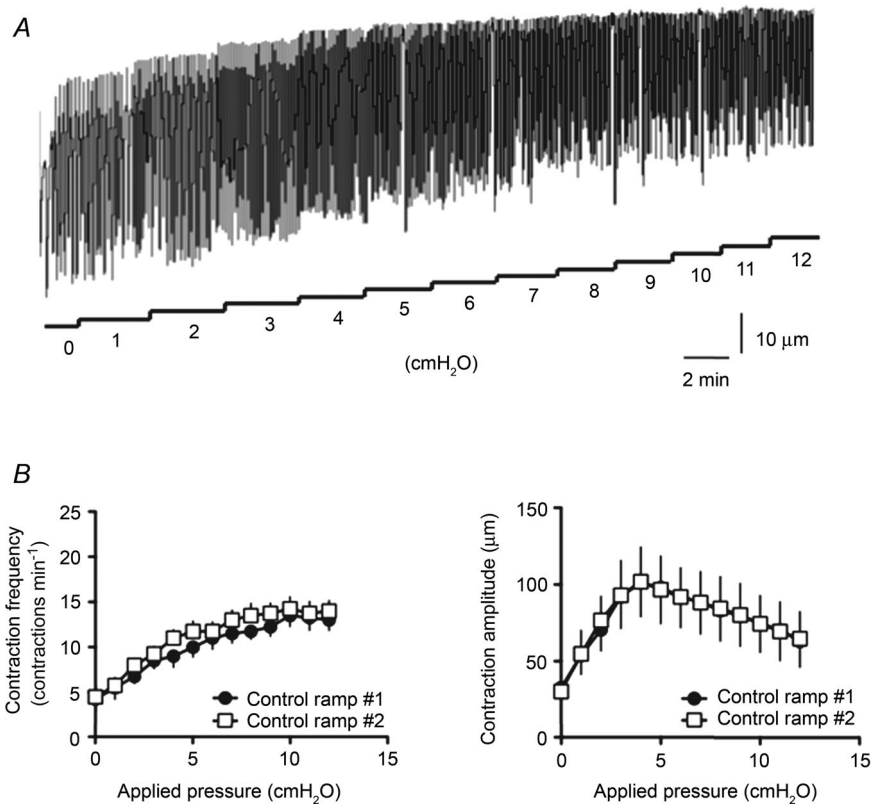

Figure 1. Effects of increase in luminal pressure on lymphatic vessel contractile function
A, original recording illustrating the changes in frequency and amplitude of lymphatic contractions in response to increase in applied pressure. *B*, step increase in pressure caused an increase in contraction frequency (left) and an initial increase in contraction amplitude followed by a decrease in amplitude as applied pressure reached values higher than 5 cmH_2O (right). Neither response was affected by a second experimental step increase in pressure.

($n = 4$; Fig. 1). The lymphatic vessels responded to a second sequential increase in luminal pressure in similar way and no significant differences were observed between two successive protocols (Fig. 1*B*).

To further assess the effect of wall stretch on lymphatic vessel contractile activity, rat mesenteric lymphatic vessels were mounted on a wire myograph and exposed to a stepwise increase in preload. As the applied tension was increased from 0 to 0.4 mN in steps of 0.05 mN, contraction frequency and the force generated by the vessel for each contraction increased to a maximum contraction frequency of 15 ± 1 contractions min^{-1}, and a force of 0.65 ± 0.1 mN ($n = 4$; Fig. 2). A subsequent second stepwise increase in preload did not lead to significant differences in the changes of contraction frequency and force (Fig. 2*B*).

Role of L-type calcium channels on pressure-induced increase in lymphatic vessel contractions

To assess the role of L-type Ca^{2+} channels in the lymphatic vessel response to pressure, we repeated the pressure increase protocol in the presence of nifedipine. At concentrations higher than 500 nM, the L-type Ca^{2+} channel blocker completely inhibited lymphatic contractions (data not shown; Azuma *et al.* 1977; Van Helden, 1993; von der Weid *et al.* 2008). Therefore, we used a lower concentration of 300 nM to observe its effects on the vessel contractile properties. Nifedipine did not markedly alter the pressure-induced increase in contraction frequency, but significantly reduced the amplitude of contractions (Fig. 3*A* and *B*). However, this inhibitory effect did not increase with increase in pressure. Similar effects were seen upon administration of 75 nM diltiazem (Fig. 3*C*).

Role of L-type calcium channels on preload-induced increase in lymphatic vessel contractions

The effects of nifedipine (100 nM) and diltiazem (75 nM) on lymphatic contractile activity were then assessed during stepwise increase in preload. These L-type Ca^{2+} channel blockers significantly reduced the stretch-induced increase in force, but did not cause any significant change in contraction frequency (Fig. 4). The inhibitory effect on contraction force did not vary with increase in preload.

Role of T-type calcium channels on pressure-induced increase in lymphatic vessel contractions

We next examined the role of T-type Ca^{2+} channels in the increase of pressure-induced changes in lymphatic vessel contractile activity. Due to the moderate selectivity of T-type Ca^{2+} channel blockers, we used two different blockers, Ni^{2+} and mibefradil at concentrations of 100 μM and 100 nM, respectively. Both Ni^{2+} and mibefradil significantly reduced the pressure-induced increase in contraction frequency, an inhibition that was not dependent on the level of pressure. The amplitude of

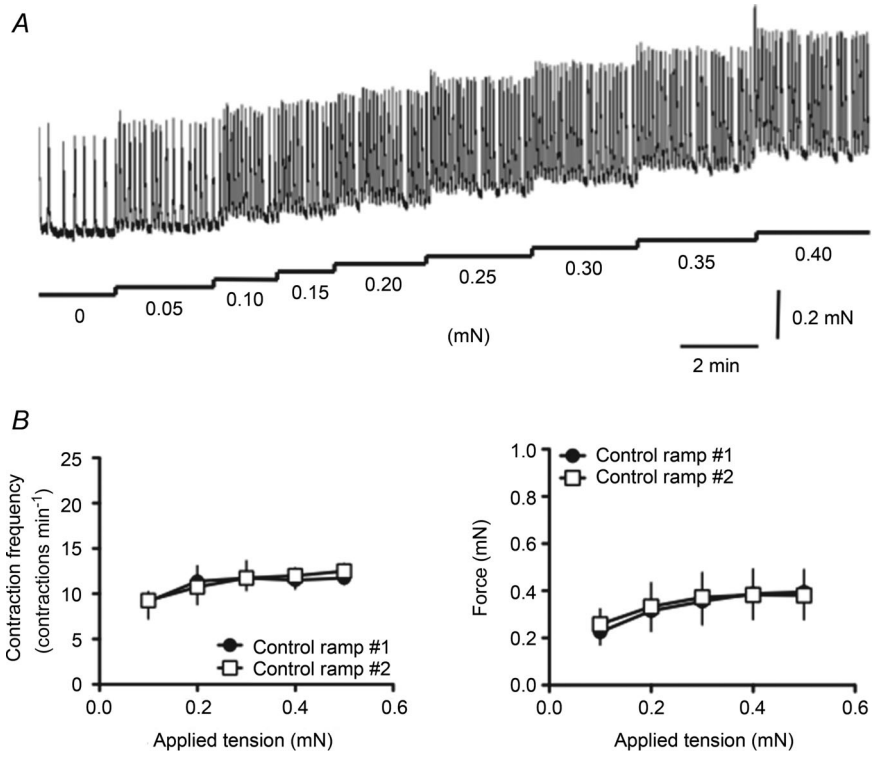

Figure 2. Effects of increase in applied tension on lymphatic vessel contractile activity
A, original recording illustrating the changes in frequency and force of lymphatic contractions in response to increase in applied tension. *B*, step increase in tension caused an increase in contraction frequency (left) and an increase in generated force (right). Both parameters reached a plateau at higher tensions. Neither response was affected by a second experimental step increase in tension.

Table 1. Nested PCR primer sequences

Gene	External/Internal	Forward (5′→3′)	Reverse (5′→3′)	Size (bp)	T_m (°C)
$Ca_v1.1$	External	CTTCCAGGTGTGAGGCCTAT	AGCTGGTTGGATGGAGTGAC	309	55
	Internal	CCAGCTGCATGGACTGAGTA	CCTGCTTCTTGCTGGTAAGG	102	55
$Ca_v1.2$	External	GCAGTATGGGAAACCCAAGA	AAAAAGCCCTACAACCACGA	373	54
	Internal	TCTGCTCTGCCTGACTCTGA	CACACAATTGGCAAAAATCG	109	54
$Ca_v1.3$	External	CATGTCCAAAGGCCTTCAAT	AGCTGCTCGTCTCCTGACTC	323	54
	Internal	TCCAGCAGGAAATTCGGTGTGTCA	TCGGTCGTGCTTGTAGGAGTAATG	187	67
$Ca_v1.4$	External	GTATCATGGCCTACGGTGGT	CCACCTTCTCCTTGGGTACA	366	57
	Internal	GCCATTGCTGTGGATAACCT	CTCCACCAGGCACCAATACT	118	56
$Ca_v3.1$	External	AACGTCCTGCTGCTCTGTTT	AGGAGTGAGCGTCCATTACG	469	55
	Internal	GCAACACCACCTGTGTCAAC	GATCCAGGCATAGCCAATGT	110	56
$Ca_v3.2$	External	AGCATCTGACTGTCCCCAAC	AACAACCTCAATGCCAAAGC	325	55
	Internal	CTGCCCAGAGAAGGAACAAG	CAGGCTCATCTCCACTGTCA	110	57
$Ca_v3.3$	External	CATCCGTATCATGCGTGTTC	GTGAGCACGAAGCTCACAAA	399	55
	Internal	CTGGTCTGCAATGACGAGAA	CCATTCCAGTTATCGCCTGT	116	55

The table shows forward and reverse primer sequences, size of the target gene and annealing temperature (T_m) of external and internal primers for rat L- and T-type Ca^{2+} channel isoforms.

contractions was, however, not markedly affected by the treatments (Fig. 5).

Role of T-type calcium channels on preload-induced increase in lymphatic vessel contractions

The effect of T-type Ca^{2+} channel blockers were then examined on a segment of lymphatic vessels mounted on the wire myograph. In these conditions, Ni^{2+} and mibefradil significantly reduced the preload-induced increase in contraction frequency without significantly affecting the force of contractions (Fig. 6). Again, the level of inhibition was independent of preload.

Effects of L- and T-type calcium channel blockers on lymphatic muscle membrane potential

We examined the contribution of L- and T-type Ca^{2+} channels on lymphatic muscle V_m in vessel segments mounted on the wire myograph. Measurements obtained from the muscle layer of the lymphatic vessels revealed regularly occurring AP-like spikes initiating the rhythmical contractions. In these control conditions, V_m values measured between APs ranged from −35 to −45 mV (mean -39 ± 2 mV, $n = 10$). Consistent with the abolition of contractions described above, administration of micromolar concentrations of nifedipine eliminated APs. This effect was consistently associated with a depolarization (~5 mV, data not shown, von der Weid *et al.* 2014). Using concentrations of nifedipine and diltiazem (300 and 75 nM, respectively) similar to the concentrations applied to assess the role of L-type Ca^{2+} channels on stretch-induced contractions, we observed no change in AP frequency (Fig. 7*A* and *C*). However, blocking T-type Ca^{2+} channels with 100 μM Ni^{2+} or 100 nM mibefradil caused a marked decrease in AP frequency correlating with a decrease in contraction rate, as described above (Fig. 7*B* and *C*). In these experimental conditions, no significant changes in resting V_m were observed in the presence of either L- or T-type Ca^{2+} channel blockers ($n = 4$, $P > 0.05$; Fig. 7*D*).

To better evaluate the contribution of VDCCs to resting V_m without the confounding consequences of stretch and endothelial damage inherent to the wire myography system (von der Weid *et al.* 2014), we further examined the effects of the blockers on lymphatic vessels pinned down to the bottom of the recoding chamber via its surrounding mesentery and as such it remained in its unstretched condition (see von der Weid *et al.* 2008, 2014). V_m values obtained from the muscle layer in these vessels were characteristically more polarized than those from wire myograph-mounted vessels, reaching −55 to −65 mV (mean -61 ± 2 mV, $n = 10$; see von der Weid *et al.* 2014). In these conditions, no significant changes were observed in the presence of nifedipine (300 nM, Fig. 8*B*). Ni^{2+} (100 μM) and mibefradil (100 nM), by contrast, consistently hyperpolarized the lymphatic muscle V_m (Fig. 8).

Expression of L- and T-type calcium channel mRNA isoforms in rat mesenteric lymphatic vessels

We investigated the presence of L- and T-type Ca^{2+} channel isoforms at the mRNA level using nested PCR (Fig. 9). Three of the four L-type Ca^{2+} channel isoforms ($Ca_v1.1$, 1.2 and 1.3) and two of the three T-type Ca^{2+} channel isoforms ($Ca_v3.1$ and 3.2) were shown to be expressed in rat mesenteric lymphatic vessels.

Immunodetection of L- and T-type calcium channel proteins in rat mesenteric lymphatic vessels

To further assess expression of the channels at the protein level, we investigated the presence of calcium channel isoforms using antibodies commercially available, in whole mount preparations of rat mesenteric lymphatic vessels by confocal immunofluorescence microscopy. Muscle cells were labelled with α-actin antibody and nuclei with DAPI. First, $Ca_v1.2$-positive staining was revealed in the lymphatic vessel wall, which appeared to co-localize with α-actin ($n = 4$; Fig. 10*A*). $Ca_v3.2$-positive staining was also detected in the vessel wall possibly co-localizing with α-actin ($n = 4$, Fig. 10*B*).

The selectivity of $Ca_v1.2$ and $Ca_v3.2$ antibodies for their respective antigen was further confirmed using HEK cells transfected with either $Ca_v1.2$ or $Ca_v3.2$ cDNA. $Ca_v1.2$ staining was detected in $Ca_v1.2$-transfected HEK cells ($n = 4$) and when cross-labelled with $Ca_v3.2$ antibodies

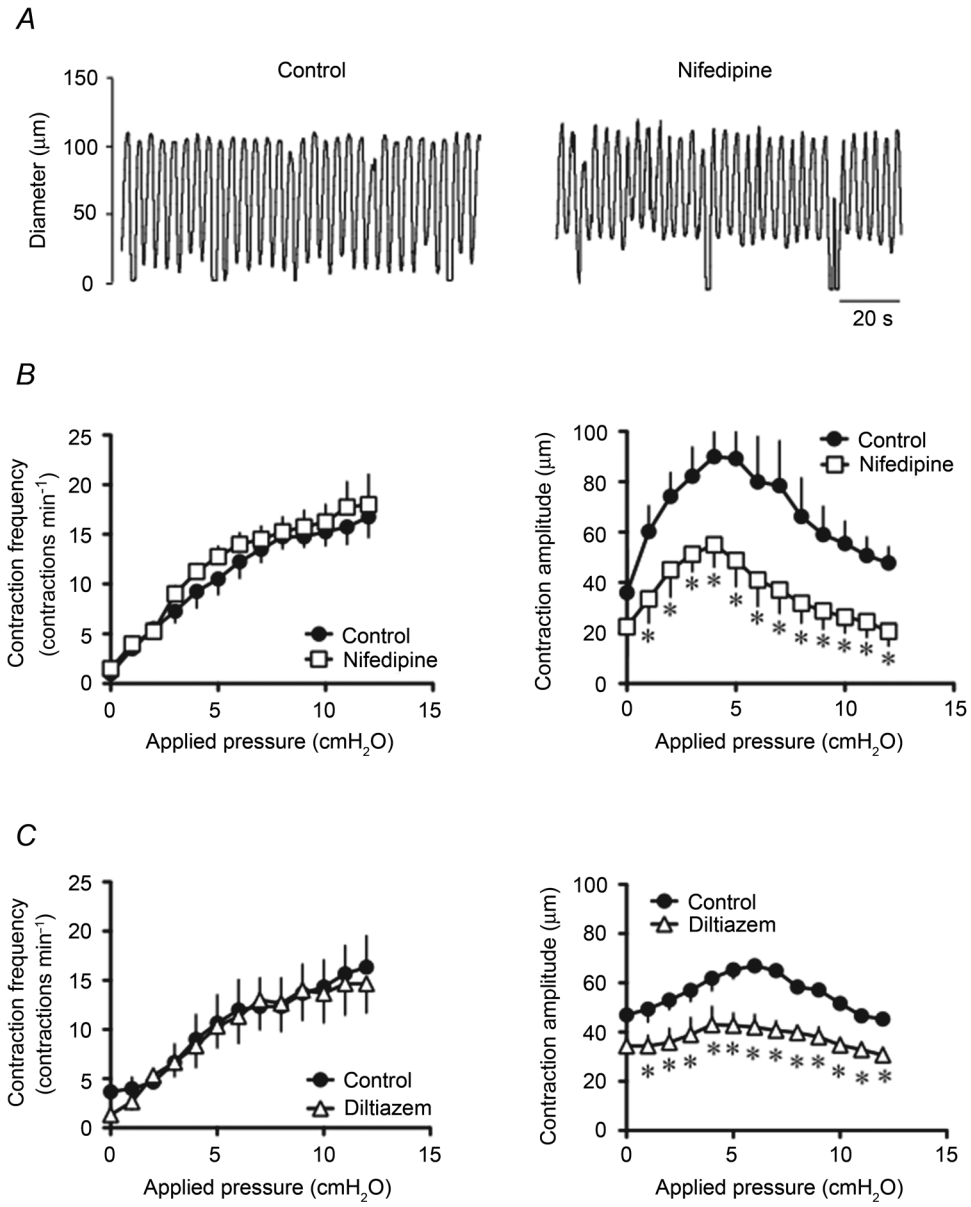

Figure 3. Effects of L-type Ca^{2+} channel blockers on the contractile activity of pressurized lymphatic vessels
A, original recording of the effect of nifedipine (300 nM) administered to a vessel at a luminal pressure of 3 cmH_2O. *B*, nifedipine had no effect on the increase in contraction frequency at any applied pressure (left), but significantly reduced the contraction amplitude (right). *C*, likewise, the other L-type Ca^{2+} channel blocker diltiazem (75 nM) did not alter the frequency–pressure relationship (left), but significantly decreased the amplitude–pressure relationship (right) ($n = 4$, $^*P < 0.05$).

no fluorescence was detected ($n = 4$; data not shown). Similarly, fluorescence was detected in $Ca_v3.2$-transfected HEK cells when labelled with $Ca_v3.2$ antibodies ($n = 4$; data not shown), but not when cross-labelled with $Ca_v1.2$ antibodies ($n = 4$; data not shown). Negative controls were also performed with non-transfected HEK cells ($n = 4$; data not shown).

Discussion

While it has been acknowledged for decades that the lymphatic system is critical for important bodily functions by transporting lymph back to the bloodstream thanks to intrinsic phasic contractions of collecting lymphatic vessels, our understanding of the ionic processes that generate as well as regulate phasic lymphatic vessel contractions is lacking. Furthermore, while we know that this contractile function is promoted by increased lymph filling and thus increase in luminal pressure and distension of the lymphatic vessel chambers, the ionic processes driving this stretch-dependent mechanism are largely unknown.

By regulating extracellular Ca^{2+} entry in smooth muscle cells, VDCCs are critical contributors of contraction. Although expression of VDCCs in lymphatics and their

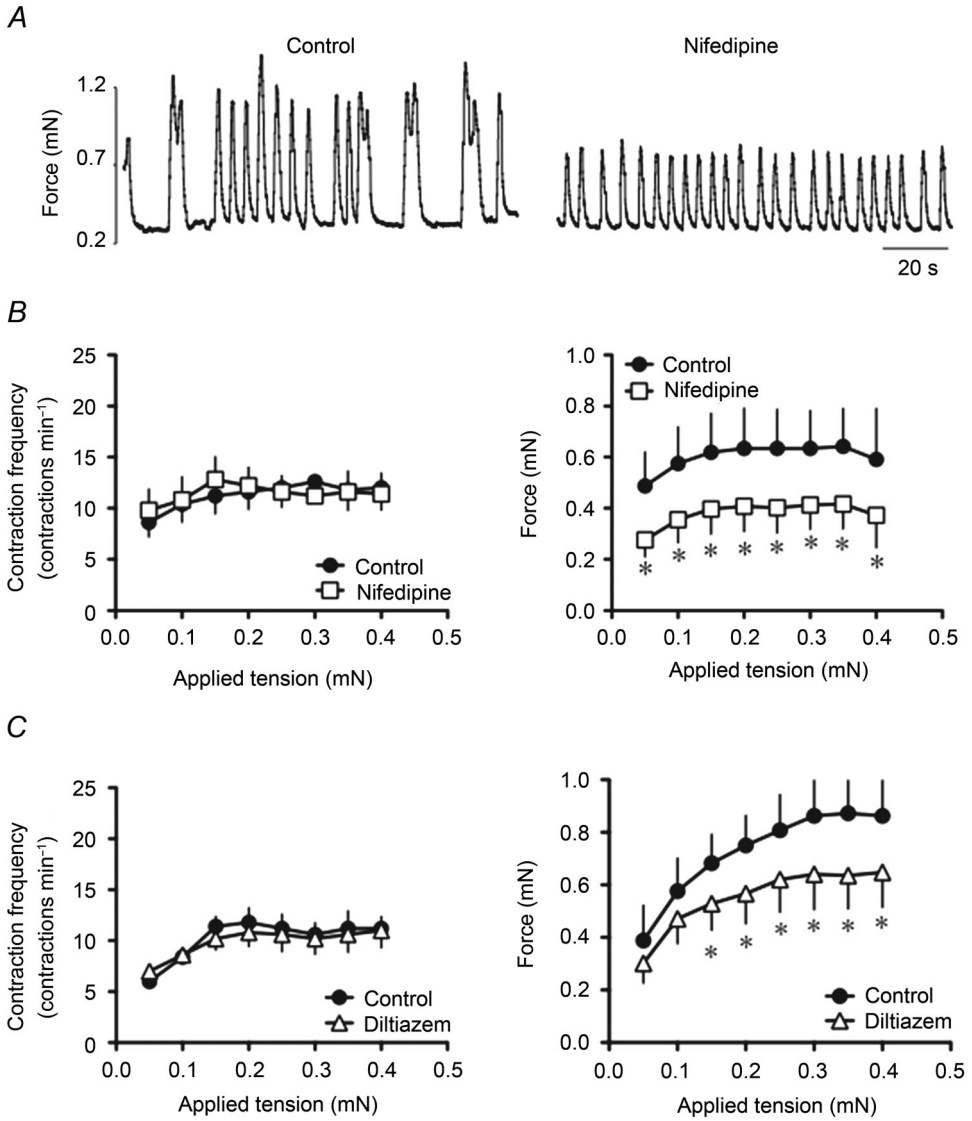

Figure 4. Effects of L-type Ca^{2+} channel blockers on the contractile activity of wire myograph-mounted lymphatic vessels
A, original recording of the effect of nifedipine (300 nM) administered to a vessel at a preload of 0.2 mN. *B*, nifedipine had no effect on the increase in contraction frequency at any applied tension (left), but significantly reduced the force generated per contraction (right). *C*, similarly, diltiazem (75 nM) did not alter the contraction frequency (left), but significantly decreased the contraction force (right) ($n = 4$–5, $^*P < 0.05$).

participation in pumping has been inferred (Azuma *et al.* 1977; McHale *et al.* 1987; Atchison & Johnston, 1997; Hollywood *et al.* 1997), a detailed characterization of the expression profile and function of VDCC members in these vessels is lacking. Our findings confirm the presence of L-type Ca^{2+} channels in rat mesenteric lymphatic vessels and suggest that they are involved in generating force and therefore regulating the amplitude of contractions. Importantly, we provide evidence that T-type Ca^{2+} channels are also expressed in rat mesenteric lymphatics and that they regulate the frequency of contraction, thus potentially contributing to the pacemaking mechanisms of lymphatic vessels. Furthermore, our functional data are confirmed by the demonstration that several members of the L- and T-type Ca^{2+} channel subfamilies are expressed at the mRNA and protein level in rat mesenteric lymphatic vessels, specifically in the lymphatic muscle cells.

L-type Ca^{2+} channels play an important role in transporting extracellular Ca^{2+} ions into muscle cells (reviewed by Hofmann *et al.* 1999; Snutch *et al.* 2001; Lacinova, 2005; Catterall, 2011). This function has also been demonstrated in lymphatic vessels, where blocking L-type Ca^{2+} channels

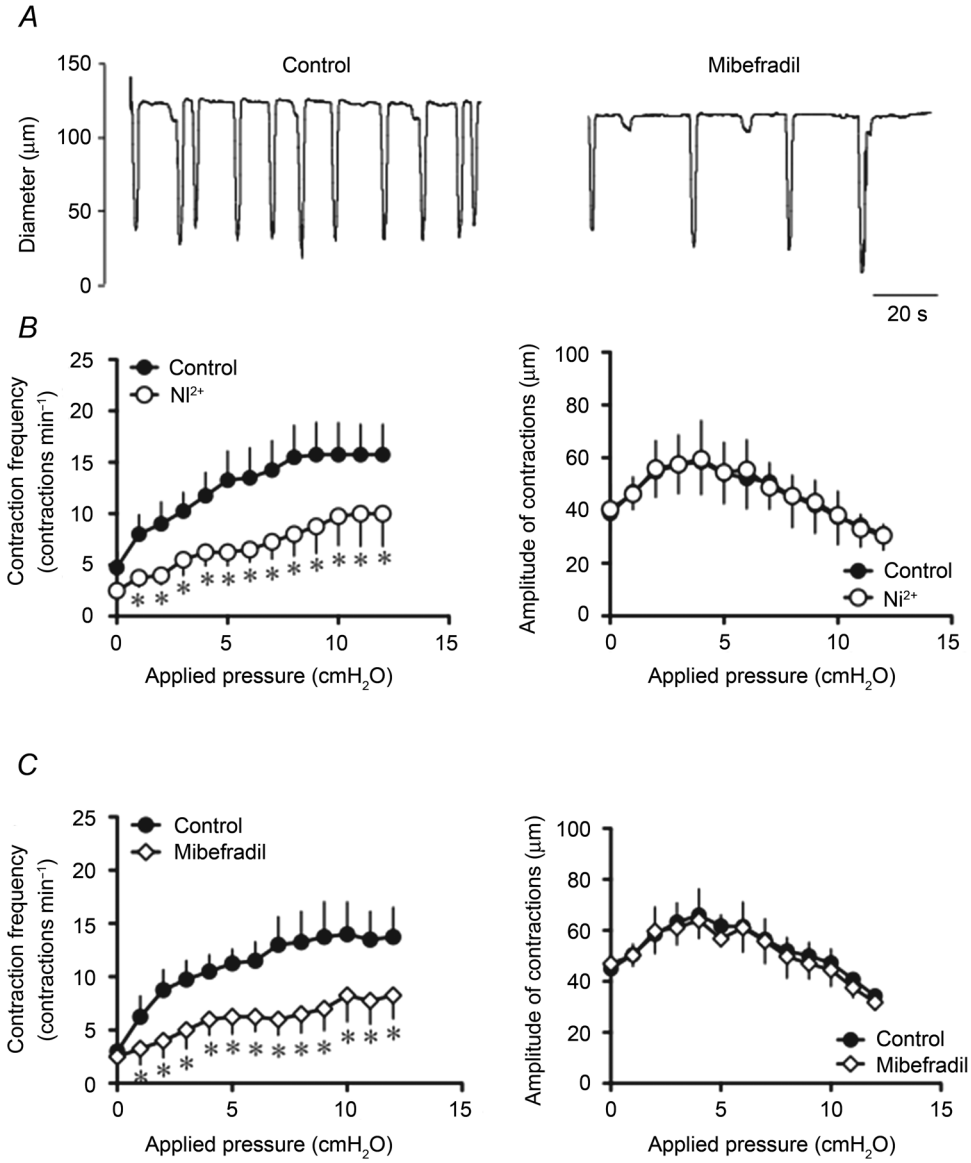

Figure 5. Effects of T-type Ca^{2+} channel blockers on the contractile activity of pressurized lymphatic vessels
A, original recording of the effect of mibefradil (100 nM administered to a vessel at a luminal pressure of 6 cmH_2O. *B*, Ni^{2+} significantly reduced the increase in contraction frequency caused by increases in applied pressure (left), but did not change the contraction amplitude (right). *C*, similarly, mibefradil (100 nM) significantly inhibited the frequency–pressure relationship (left), without affecting the force–pressure relationship (right) ($n = 4$, $^*P < 0.05$).

with high concentrations of dihydropyridines abolishes APs, Ca^{2+} entry and subsequent contractions (McHale & Allen, 1983; Atchison & Johnston, 1997; von der Weid *et al.* 2008). To further investigate the roles of these channels in lymphatic contraction and stretch activation, we use two classes of pharmacological blockers, nifedipine and diltiazem, at low concentrations to avoid abolishing the contractions while being able to examine their effects on contraction frequency and strength. Nifedipine, at concentrations higher than 1 μM, abolished contractions as well as APs, an effect similarly observed with diltiazem at a concentration higher than 500 nM (data not shown). Administration of a lower concentration (300 nM) of nifedipine to lymphatic vessels mounted on the pressure myograph resulted in a significant reduction in the contraction amplitude at each pressure step without affecting contraction frequency (Fig. 3). These findings were confirmed with wire myograph experiments, where

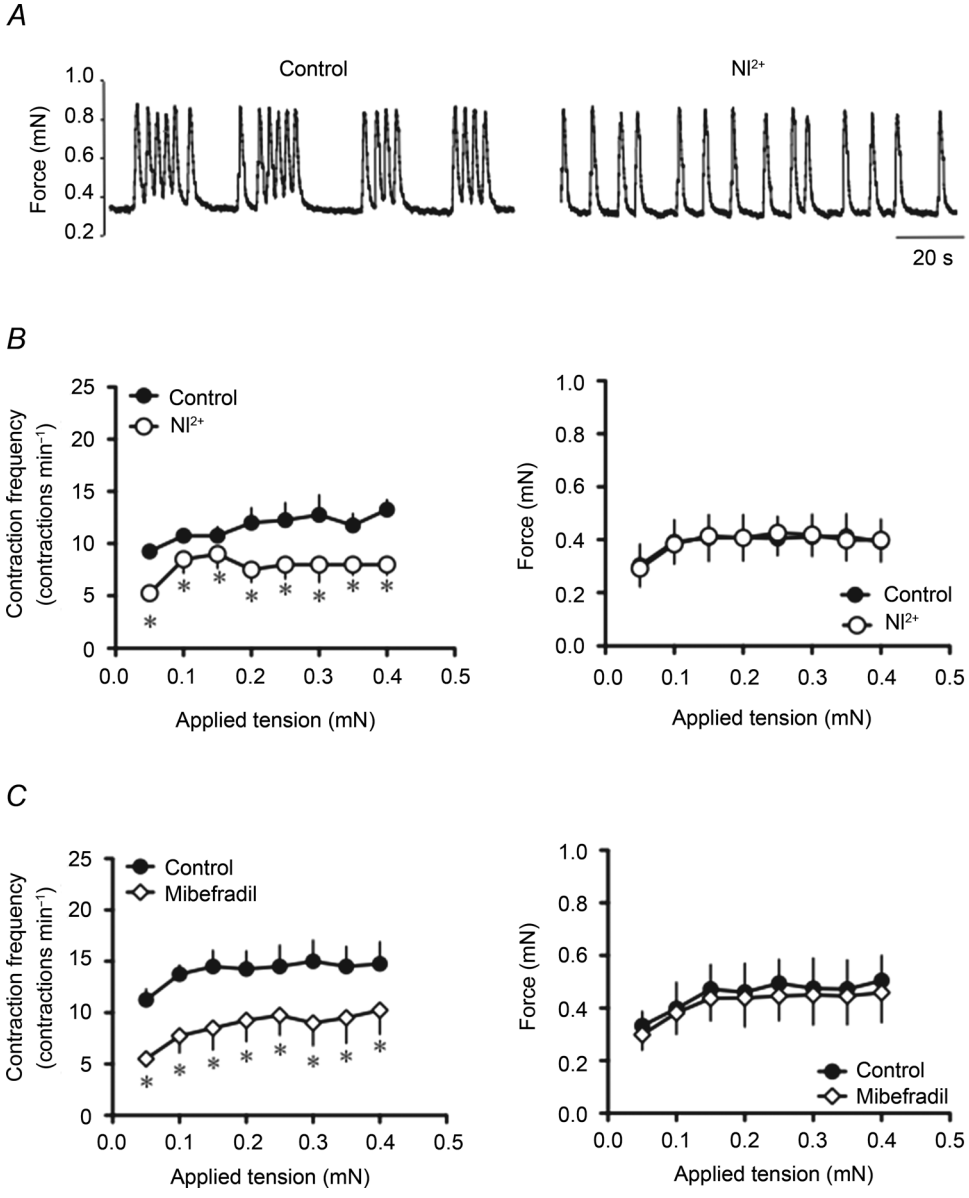

Figure 6. Effects of T-type Ca^{2+} channel blockers on contractile activity of wire myograph-mounted lymphatic vessels
A, original recording of the effect of Ni^{2+} (100 μM) administered to a vessel at a preload of 0.3 mN. *B*, Ni^{2+} significantly reduced the increase in contraction frequency caused by increases in applied tension (left), but did not change the force generated per contraction at any applied tension (right). *C*, likewise, mibefradil (100 nM) significantly decreased the contraction frequency (left graph), without affecting the contraction force (right) ($n = 4$, $^*P < 0.05$).

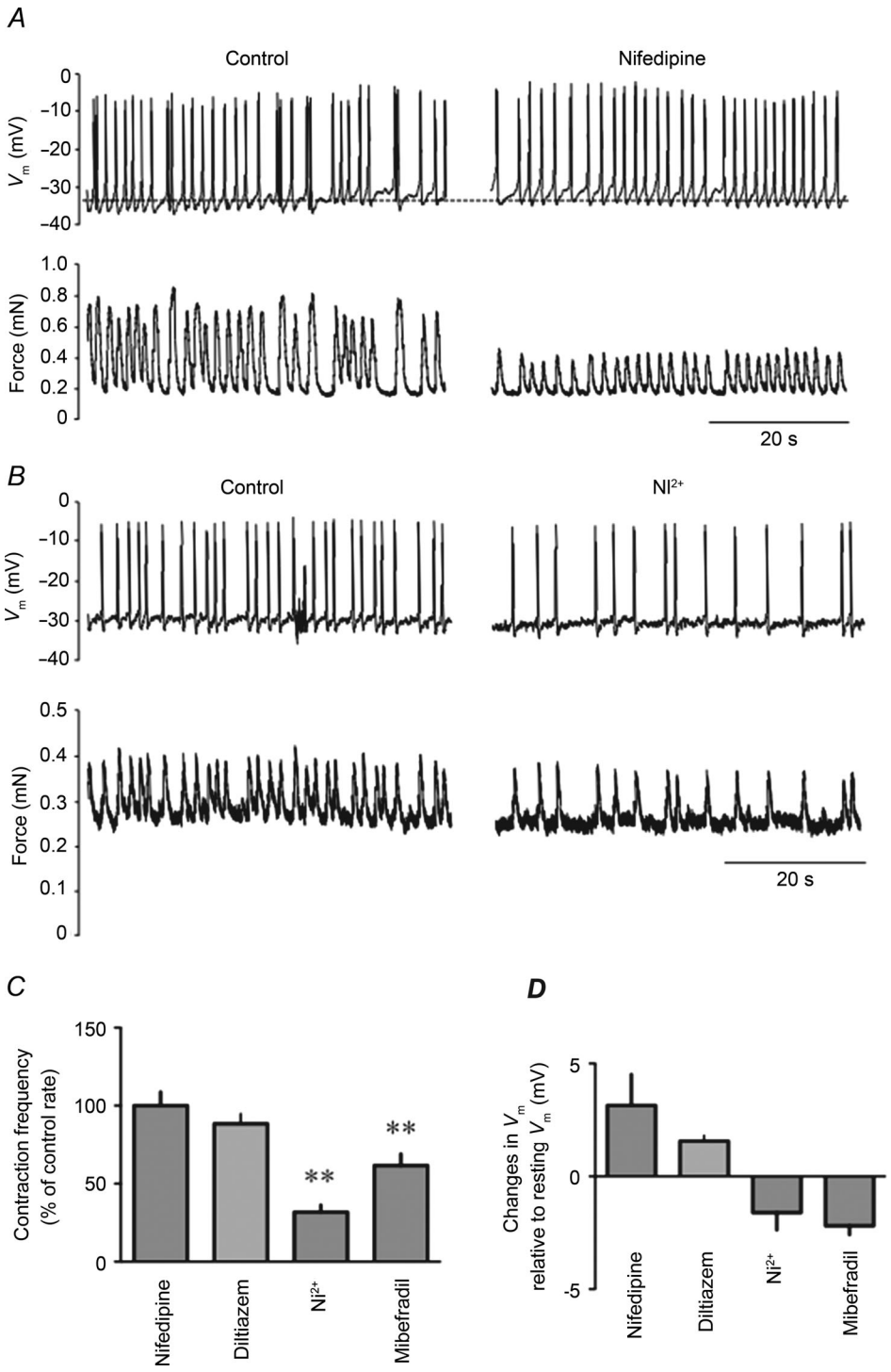

Figure 7. Effect of VDCC blockers on the lymphatic muscle membrane potential of wire myograph-mounted vessels
A and *B*, original recordings of lymphatic muscle V_m (top traces) and force (bottom traces) upon administration of nifedipine (300 nM, *A*) and Ni^{2+} (100 μM, *B*). Upward deflections denote depolarization (top) and contraction (bottom) leading to AP and force generation, respectively. *C*, summary bar graph of VDCC blocker effects on AP frequency. Data are expressed as percentage changes compared to control frequencies (nifedipine, 300 nM, $n = 4$; diltiazem, 75 nM, $n = 3$; Ni^{2+}, 100 μM, $n = 4$; mibefradil, 100 nM, $n = 4$, $^{**}P < 0.01$). *D*, summary bar graph of V_m changes caused by VDCC blockers during the same experiments. Data are expressed as the calculated differences between V_m in control condition and V_m in the presence of the blocker.

both nifedipine and diltiazem significantly reduced the contractile force at each applied tension step, while not affecting contraction frequency (Fig. 4). We used a higher concentration of nifedipine for the pressure myography experiments (300 nM compared to 100 nM during wire myography) to accommodate the light sensitivity of nifedipine (Majeed *et al.* 1987) as light was required to track the diameter of the lymphatic vessel. As demonstrated by Zhang *et al.* (2007), isometric and isobaric methods used in this study yield qualitatively similar indices of lymphatic contractile activity and while contractile force and contraction amplitude cannot be directly correlated, it could be presumed that less force would result in lower amplitude of contractions. Although detailed mechanisms involved in the development of contraction strength need to be investigated further, our data are consistent with L-type Ca^{2+} channels regulating extracellular Ca^{2+} entry into the lymphatic muscle cells, thereby increasing the availability of cytosolic Ca^{2+} to drive contraction strength.

Pharmacological identification of T-type Ca^{2+} channels in smooth muscles has been limited by the lack of highly selective pharmacological blockers and many suitable drugs have been shown to also affect other ion channels. In our study, we used Ni^{2+} and mibefradil, two drugs widely used to investigate T-type Ca^{2+} channels in smooth muscle. To selectively favour the inhibition of T-type Ca^{2+} channels without other confounding actions, low concentrations were used as investigated in various studies (Bezprozvanny & Tsien, 1995; Clozel *et al.* 1997; McDonough & Bean, 1998; Hobai *et al.* 2000; Martin *et al.* 2000; Diaz *et al.* 2005). The similar results obtained with the two pharmacological blockers in both pressure and wire myography experiments further support the selective inhibition of T-type Ca^{2+} channel action in our experimental conditions. Application of 100 μM Ni^{2+} and 100 nM mibefradil decreased contraction frequency at each increase in tension or luminal pressure step, without affecting the amplitude or force of contractions (Figs 5 and 6). Use of higher concentrations (500 μM Ni^{2+} and 1 μM mibefradil) caused a total abolition of contractions (P. Y. von der Weid, unpublished data), probably due to the action of the blockers on other molecular targets (Gomora *et al.* 1999; Lee *et al.* 1999*b*; Hobai *et al.* 2000; Heady *et al.* 2001; Moosmang *et al.* 2006).

Microelectrode recordings from a segment of lymphatic vessel mounted on a wire myograph confirmed that each contraction is preceded by an L-type Ca^{2+} channel-driven AP, which can also be abolished by micromolar concentrations of nifedipine (Azuma *et al.* 1977; McHale *et al.* 1987; Atchison & Johnston, 1997; Hollywood *et al.* 1997). Lower concentrations of nifedipine or diltiazem caused a decrease in contractile force, but had no effect on AP frequency. Our data further suggest that L-type Ca^{2+} channels may not play a significant role in setting the lymphatic muscle resting V_m, as nifedipine and diltiazem caused no significant change in lymphatic muscle V_m, whether recordings were obtained under the stretch provided by the separation of the wires or from unstretched lymphatic vessels. L-type Ca^{2+} channels, however, have been shown to play a role in shaping the AP in other electrically active smooth muscle cells such as in the urinary bladder and the colon, where they were reported to mediate the upstroke of APs (Bywater *et al.* 1989; Heppner *et al.* 1997). Further in-depth investigations of the contribution of these channels to electrical activity of lymphatic contractions are required.

Assessing the role of T-type Ca^{2+} channels on modulating lymphatic muscle V_m in stretched lymphatic vessels mounted on the wire myograph and unstretched vessels garnered slightly different results. Specifically, administration of either Ni^{2+} or mibefradil on unstretched vessels where lymphatic muscle V_m ranged from

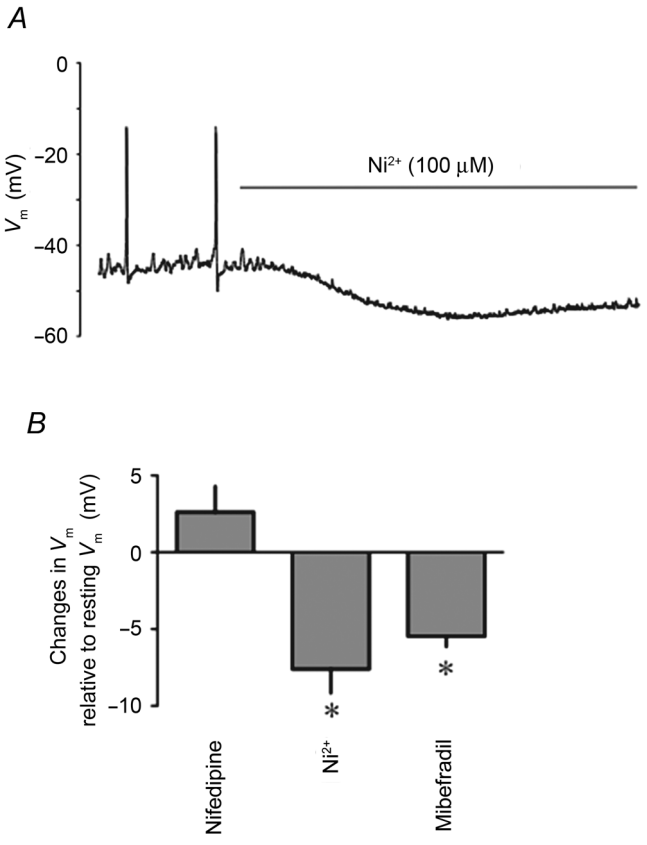

Figure 8. Effect of VDCC blockers on membrane potential of unstretched lymphatic muscle
A, original smooth muscle V_m recording in an unstretched rat mesenteric lymphatic vessel illustrating the effect of Ni^{2+} (100 μM). *B*, summary bar graph of V_m changes caused by VDCC blockers nifedipine (300 nM), Ni^{2+} (100 μM) and mibefradil (100 nM). Data are expressed as the calculated differences between V_m in control condition and V_m in the presence of the blocker ($n = 4$, $^*P<0.05$).

−55 to −65 mV revealed a significant hyperpolarization, suggesting contribution of the channels to the resting V_m. Indeed, T-type Ca^{2+} channels are classified as low voltage activation channels, and are activated at polarized membrane potentials (Hirano *et al.* 1989). On the other hand, superfusion with the blockers of lymphatic vessel segments mounted on the wire myograph where muscle cells are more depolarized (−35 to −45 mV, also see von der Weid *et al.* 2014) led to no significant changes in V_m. However, in the same conditions, T-type channel blockers caused a decrease in contraction frequency, suggesting contribution of the channels. It is possible that the stretch of the vessel wall in the wire-myography experiments activates a collection of depolarizing ion conductances, among them T-type Ca^{2+} channels, involved in modulation of AP/contraction frequency. Inhibition of one of these channels, such as T-type Ca^{2+} channels, would lead to lower frequency, but would not necessarily affect V_m. Of note is the observation that in the same preparation, step increase in stretch caused no changes in V_m associated with an increase in AP/contraction frequency (von der Weid *et al.* 2014). The involvement of T-type Ca^{2+} channels in the regulation of V_m in unstretched vessels and in the frequency of lymphatic contractions strongly suggests their participation to the pacemaking mechanism of lymphatic pumping (Beckett *et al.* 2007; von der Weid *et al.* 2008). Similar to our findings, T-type Ca^{2+} channels have also been reported to modulate electrical activity in other smooth muscles, such as rabbit urethra and guinea pig detrusor muscle of the urinary bladder, where their inhibition led to a decrease in frequency of APs (Bradley *et al.* 2004; Yanai *et al.* 2006). Moreover, a role for T-type Ca^{2+} channels in the pacemaking mechanism of the heart has been demonstrated, as blocking T-type Ca^{2+} channels in the sino-atrial node has been reported to slow the cardiac diastolic depolarization, also referred to as the 'pacemaker potential' (Zhou & Lipsius, 1994; Huser *et al.* 2000). Further investigations are required to determine the specific role of T-type Ca^{2+} channels in the generation of APs leading to lymphatic contractions.

Investigations to determine which family members of L- and T-type Ca^{2+} channels were expressed in mesenteric lymphatic vessels revealed using nested PCR

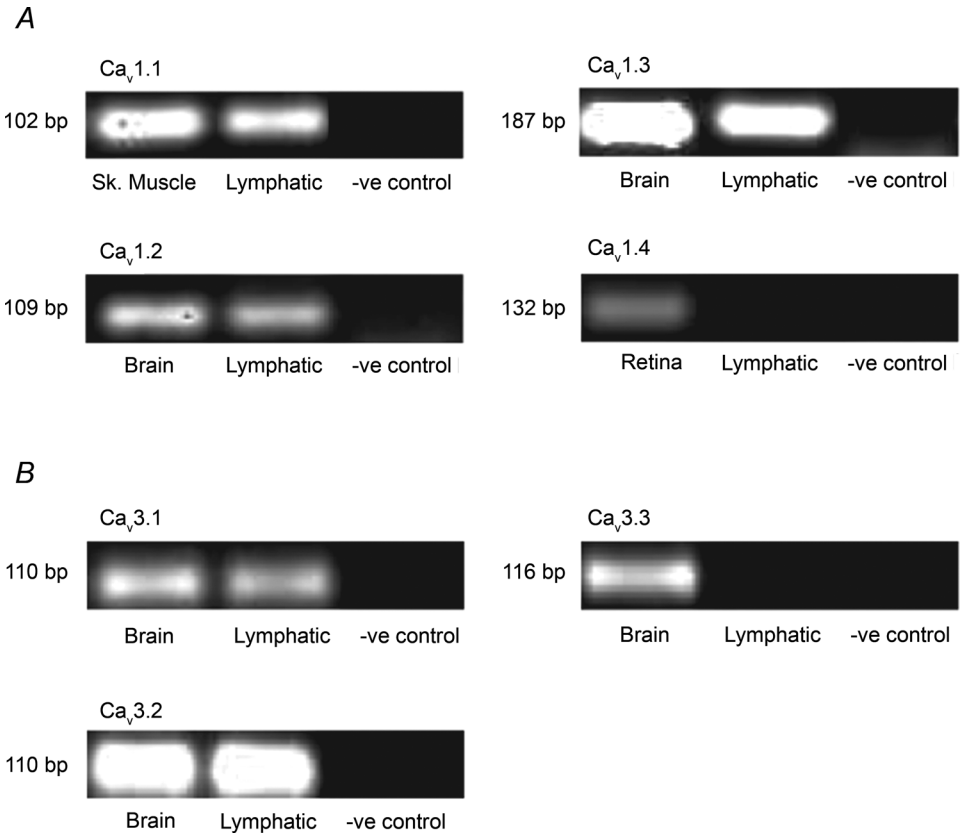

Figure 9. Expression of L- and T-type Ca^{2+} channel mRNAs in rat mesenteric lymphatic vessels
Agarose gel images of lymphatic nested PCR products amplified from sets of primers for α_1 pore-forming subunits of L- and T-type Ca^{2+} channels ($Ca_v1.1$–1.4 and Ca_v 3.1–3.3, respectively). Rat brain, retina and skeletal muscle were used as positive control tissues and negative controls were performed in the absence of cDNA. Data shown are representative of four similar experiments.

that three of the four members of the L-type Ca^{2+} channel family ($Ca_v1.1$, 1.2 and 1.3) and two of the three members of the T-type Ca^{2+} channel family ($Ca_v3.1$ and 3.2) were expressed in rat mesenteric lymphatics at the mRNA level. Most of these isoforms ($Ca_v1.2$, 1.3, 3.1 and 3.2) are expressed in smooth and cardiac muscle (Mikami *et al.* 1989; Biel *et al.* 1990; Seino *et al.* 1992; Cribbs *et al.* 1998; Benardeau *et al.* 2000; Pignier & Potreau, 2000; Gustafsson *et al.* 2001; Feng *et al.* 2004). In particular and with relevance to lymphatic pumping, $Ca_v1.3$, 3.1 and 3.2 are classically expressed in the sino-atrial node where they have been proposed to be involved in heart pacemaking (Seino *et al.* 1992; Ono & Iijima, 2005) and $Ca_v3.1$ transcripts have been identified in smooth muscle tissues with phasic contractile activity, such as the urethra, urinary bladder and

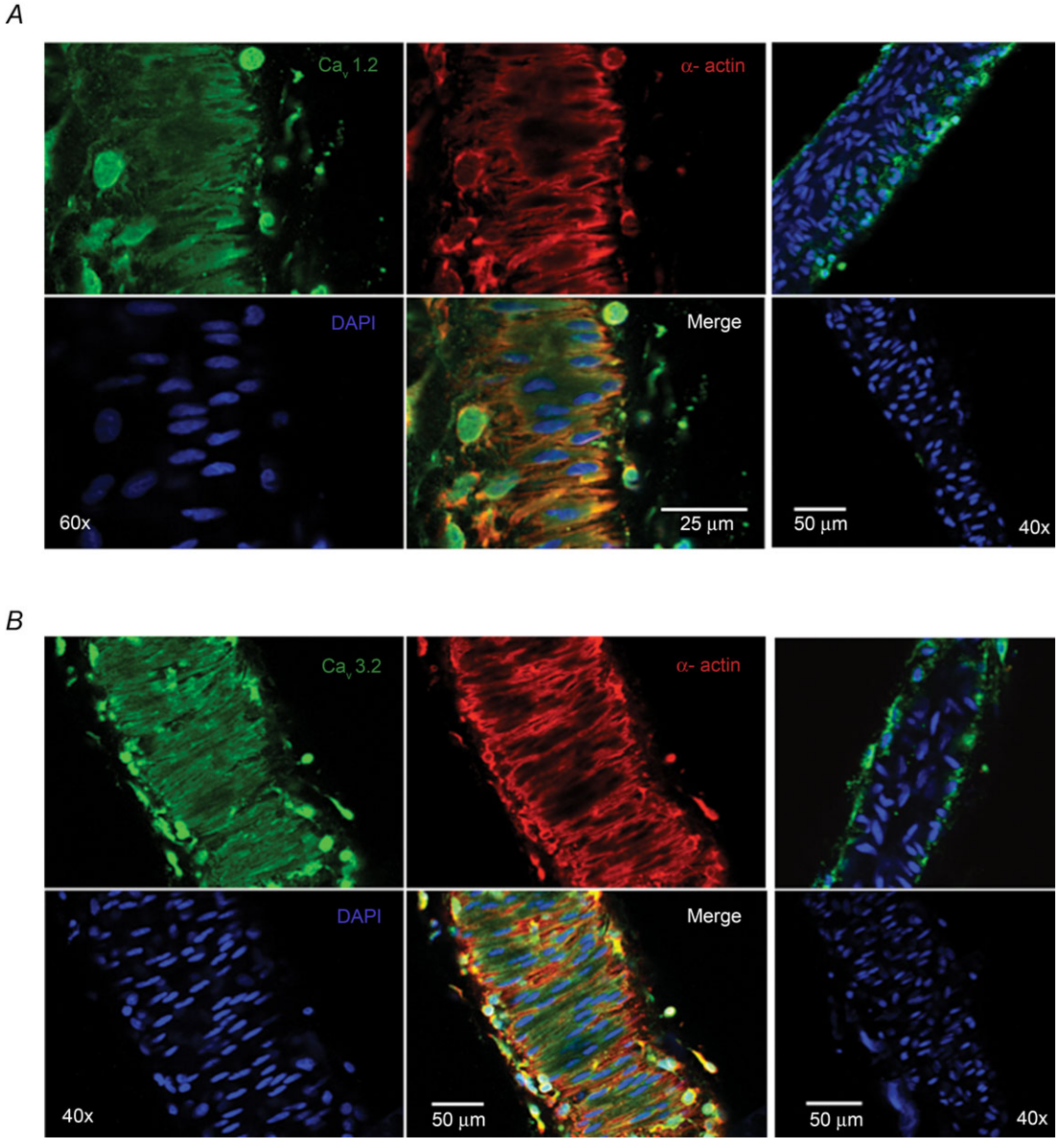

Figure 10. Immunolocalization of $Ca_v1.2$ and $Ca_v3.2$ in rat mesenteric lymphatic vessels
Confocal photomicrographs of whole mount rat lymphatic vessels. Images show immunoreactivity (green) for $Ca_v1.2$ (*A*, 60× magnification) and $Ca_v3.2$ (*B*, 40× magnification), α-actin (red) to identify the lymphatic muscle cells, and DAPI (blue) to stain nuclei. Merge images suggest that the expression of L- and T-type Ca^{2+} channels is mostly located in lymphatic muscle. Negative controls (40× magnification) are presented in the right-hand side of the figure, the top images illustrating incubation with $Ca_v1.2$ and $Ca_v3.2$ immunopeptides (*A* and *B*, respectively), while bottom images were obtained in the absence of primary antibody. DAPI staining is also shown to confirm vessel orientation. Note that these vessels are constricted, and therefore they present a smaller diameter. Images are representative of three experiments for each Ca^{2+} channel antibody.

uterus (Young *et al.* 1993; Lee *et al.* 1999*a*; Sui *et al.* 2001). $Ca_v1.1$, by contrast, is predominantly expressed in the skeletal muscle (Tanabe *et al.* 1987). These findings further highlight the uniqueness of the lymphatic muscle and align well with other studies reporting expression of smooth muscle, cardiac and skeletal contractile proteins in rat mesenteric lymphatic vessels (Muthuchamy *et al.* 2003). We supplemented our mRNA data by investigating the expression and localization of VDCCs at the protein level using commercially available $Ca_v1.2$ and 3.2 antibodies detected by immunofluorescence imaging. Our results show co-localization of $Ca_v1.2$ and 3.2 antibodies using α-actin staining, indicating expression of $Ca_v1.2$ and 3.2 channels in the muscle cells. α-Actin, present in a variety of muscle cells as a major component in the contractile apparatus, was used to identify lymphatic muscle cells. Controls using $Ca_v1.2$- and 3.2-transfected HEK cells validate the selectivity of antibodies (data not shown).

At the molecular and functional levels, our data demonstrate the presence of L- and T-type Ca^{2+} channels in lymphatic vessels. Only a handful of studies have previously suggested T-type Ca^{2+} channel expression in the muscles of lymphatic vessels. Hollywood *et al.* (1997) and Convery *et al.* (1997) reported in abstract forms the identification of T-type Ca^{2+} currents in freshly dissociated sheep mesenteric lymphatic muscle cells, and further demonstrated on pressurized sheep vessels a decrease in contraction frequency during Ni^{2+} incubation. Using the same lymphatic vessels mounted on a wire myograph to allow proper maintenance of microelectrode impalements and V_m recordings, Beckett *et al.* (2007) showed that Ni^{2+} alters lymphatic APs, an observation confirmed in guinea pig mesenteric lymphatic (von der Weid *et al.* 2008). We further revealed distinct roles played by T-type Ca^{2+} channels in regulating stretch-activated lymphatic contractions, where L-type Ca^{2+} channels modulate contraction strength and T-type Ca^{2+} channels regulate contraction frequency. Similar observations reported in other phasically contracting smooth muscles support the differential roles of these two VDCC subtypes in phasically contracting smooth muscle cells. Specifically in the uterine smooth muscle, nifedipine produced a decrease in the amplitude of contractions, while administration of Ni^{2+} resulted in a decrease of contraction frequency (Lee *et al.* 2009), and in the human myometrium, 100 μM Ni^{2+} decreased contraction frequency (Blanks *et al.* 2007).

Conclusion

The present study focused on investigating the expression of VDCCs in rat mesenteric lymphatic vessels and assessing their role in the regulation of lymphatic pumping. We have delineated the distinct functions of L- and T-type Ca^{2+} channels in stretch-activated lymphatic contractions and our data suggest that L-type Ca^{2+} channels are important for generating strength of contractions and play the same role in excitation–contraction coupling that they do in other smooth muscles, while T-type Ca^{2+} channels play a role in regulating lymphatic muscle V_m and contraction frequency. Further investigation is required to characterize the electrophysiological properties of VDCCs in lymphatic vessels. Additionally, expressional studies allowed us to confirm the presence of L- and T-type Ca^{2+} channels, as well as their main localization in lymphatic muscle cells. This study fosters our knowledge on the mechanisms that drive stretch-activated lymphatic contractions, and may help in providing a basis to developing therapeutic agents to enhance lymphatic function during lymphatic impairment such as lymphoedema.

References

Allen JM, McHale NG & Rooney BM (1983). Effect of norepinephrine on contractility of isolated mesenteric lymphatics. *Am J Physiol* **244**, H479–486.

Atchison DJ & Johnston MG (1997). Role of extra- and intracellular Ca^{2+} in the lymphatic myogenic response. *Am J Physiol* **272**, R326–333.

Azuma T, Ohhashi T & Sakaguchi M (1977). Electrical activity of lymphatic smooth muscles. *Proc Soc Exp Biol Med* **155**, 270–273.

Beckett EA, Hollywood MA, Thornbury KD & McHale NG (2007). Spontaneous electrical activity in sheep mesenteric lymphatics. *Lymphat Res Biol* **5**, 29–43.

Benardeau A, Weissenburger J, Hondeghem L & Ertel EA (2000). Effects of the T-type Ca^{2+} channel blocker mibefradil on repolarization of guinea pig, rabbit, dog, monkey, and human cardiac tissue. *J Pharmacol Exp Ther* **292**, 561–575.

Bezprozvanny I & Tsien RW (1995). Voltage-dependent blockade of diverse types of voltage-gated Ca^{2+} channels expressed in *Xenopus* oocytes by the Ca^{2+} channel antagonist mibefradil (Ro 40–5967). *Mol Pharmacol* **48**, 540–549.

Biel M, Ruth P, Bosse E, Hullin R, Stuhmer W, Flockerzi V & Hofmann F (1990). Primary structure and functional expression of a high voltage activated calcium channel from rabbit lung. *FEBS Lett* **269**, 409–412.

Blanks AM, Zhao ZH, Shmygol A, Bru-Mercier G, Astle S & Thornton S (2007). Characterization of the molecular and electrophysiological properties of the T-type calcium channel in human myometrium. *J Physiol* **581**, 915–926.

Bradley JE, Anderson UA, Woolsey SM, Thornbury KD, McHale NG & Hollywood MA (2004). Characterization of T-type calcium current and its contribution to electrical activity in rabbit urethra. *Am J Physiol Cell Physiol* **286**, C1078–1088.

Bywater RA, Small RC & Taylor GS (1989). Neurogenic slow depolarizations and rapid oscillations in the membrane potential of circular muscle of mouse colon. *J Physiol* **413**, 505–519.

Catterall WA (2011). Voltage-gated calcium channels. *Cold Spring Harb Perspect Biol* **3**, a003947.

Clozel JP, Ertel EA & Ertel SI (1997). Discovery and main pharmacological properties of mibefradil (Ro 40–5967), the first selective T-type calcium channel blocker. *J Hypertens Suppl* **15**, S17–25.

Convery M, Hollywood MA, Cotton KD, Thornbury KD & McHale NG (1997). Role of inward currents in pumping activity of isolated sheep lymphatics. *J Physiol* **501**, 110P–111P.

Cribbs LL, Lee JH, Yang J, Satin J, Zhang Y, Daud A, Barclay J, Williamson MP, Fox M, Rees M & Perez-Reyes E (1998). Cloning and characterization of α1H from human heart, a member of the T-type Ca^{2+} channel gene family. *Circ Res* **83**, 103–109.

Davis MJ, Donovitz JA & Hood JD (1992). Stretch-activated single-channel and whole cell currents in vascular smooth muscle cells. *Am J Physiol* **262**, C1083–1088.

Davis MJ, Lane MM, Scallan JP, Gashev AA & Zawieja DC (2007). An automated method to control preload by compensation for stress relaxation in spontaneously contracting, isometric rat mesenteric lymphatics. *Microcirculation* **14**, 603–612.

Diaz D, Bartolo R, Delgadillo DM, Higueldo F & Gomora JC (2005). Contrasting effects of Cd^{2+} and Co^{2+} on the blocking/unblocking of human Cav3 channels. *J Membr Biol* **207**, 91–105.

Dougherty PJ, Davis MJ, Zawieja DC & Muthuchamy M (2008). Calcium sensitivity and cooperativity of permeabilized rat mesenteric lymphatics. *Am J Physiol Regul Integr Comp Physiol* **294**, R1524–1532.

Duling BR, Gore RW, Dacey Jr RG & Damon DN (1981). Methods for isolation, cannulation, and *in vitro* study of single microvessels. *Am J Physiol* **241**, H108–116.

Feng MG, Li M & Navar LG (2004). T-type calcium channels in the regulation of afferent and efferent arterioles in rats. *Am J Physiol Renal Physiol* **286**, F331–337.

Fox JL & von der Weid PY (2002). Effects of histamine on the contractile and electrical activity in isolated lymphatic vessels of the guinea-pig mesentery. *Br J Pharmacol* **136**, 1210–1218.

Gashev AA, Davis MJ, Delp MD & Zawieja DC (2004). Regional variations of contractile activity in isolated rat lymphatics. *Microcirculation* **11**, 477–492.

Gomora JC, Enyeart JA & Enyeart JJ (1999). Mibefradil potently blocks ATP-activated K^+ channels in adrenal cells. *Mol Pharmacol* **56**, 1192–1197.

Gustafsson F, Andreasen D, Salomonsson M, Jensen BL & Holstein-Rathlou N (2001). Conducted vasoconstriction in rat mesenteric arterioles: role for dihydropyridine-insensitive Ca^{2+} channels. *Am J Physiol Heart Circ Physiol* **280**, H582–590.

Hagiwara N, Irisawa H & Kameyama M (1988). Contribution of two types of calcium currents to the pacemaker potentials of rabbit sino-atrial node cells. *J Physiol* **395**, 233–253.

Hargens AR & Zweifach BW (1977). Contractile stimuli in collecting lymph vessels. *Am J Physiol* **233**, H57–65.

Heady TN, Gomora JC, Macdonald TL & Perez-Reyes E (2001). Molecular pharmacology of T-type Ca^{2+} channels. *Jpn J Pharmacol* **85**, 339–350.

Heppner TJ, Bonev AD & Nelson MT (1997). Ca^{2+}-activated K^+ channels regulate action potential repolarization in urinary bladder smooth muscle. *Am J Physiol* **273**, C110–117.

Hirano Y, Fozzard HA & January CT (1989). Characteristics of L- and T-type Ca^{2+} currents in canine cardiac Purkinje cells. *Am J Physiol* **256**, H1478–1492.

Hobai IA, Hancox JC & Levi AJ (2000). Inhibition by nickel of the L-type Ca channel in guinea pig ventricular myocytes and effect of internal cAMP. *Am J Physiol Heart Circ Physiol* **279**, H692–701.

Hofmann F, Lacinová L & Klugbauer N (1999). Voltage-dependent calcium channels: from structure to function. *Rev Physiol Biochem Pharmacol* **139**, 33–87.

Hollywood MA, Cotton KD, Thorbury KD & McHale NG (1997). Isolated sheep mesenteric lymphatic smooth muscle possess both T- and L-type calcium currents. *J Physiol* **501**, 109–110.

Huser J, Blatter LA & Lipsius SL (2000). Intracellular Ca^{2+} release contributes to automaticity in cat atrial pacemaker cells. *J Physiol* **524**, 415–422.

Imtiaz MS, Zhao J, Hosaka K, von der Weid PY, Crowe M & van Helden DF (2007). Pacemaking through Ca^{2+} stores interacting as coupled oscillators via membrane depolarization. *Biophys J* **92**, 3843–3861.

Kimura M, Obara K, Sasase T, Ishikawa T, Tanabe Y & Nakayama K (2000). Specific inhibition of stretch-induced increase in L-type calcium channel currents by herbimycin A in canine basilar arterial myocytes. *Br J Pharmacol* **130**, 923–931.

Kirkpatrick CT & McHale NG (1977). Electrical and mechanical activity of isolated lymphatic vessels [proceedings]. *J Physiol* **272**, 33P–34P.

Knot HJ & Nelson MT (1995). Regulation of membrane potential and diameter by voltage-dependent K^+ channels in rabbit myogenic cerebral arteries. *Am J Physiol* **269**, H348–355.

Knot HJ & Nelson MT (1998). Regulation of arterial diameter and wall $[Ca^{2+}]$ in cerebral arteries of rat by membrane potential and intravascular pressure. *J Physiol* **508**, 199–209.

Kuo IY, Ellis A, Seymour VA, Sandow SL & Hill CE (2010). Dihydropyridine-insensitive calcium currents contribute to function of small cerebral arteries. *J Cereb Blood Flow Metab* **30**, 1226–1239.

Lacinova L (2005). Voltage-dependent calcium channels. *Gen Physiol Biophys* **24**(Suppl 1), 1–78.

Langton PD (1993). Calcium channel currents recorded from isolated myocytes of rat basilar artery are stretch sensitive. *J Physiol* **471**, 1–11.

Lee JH, Daud AN, Cribbs LL, Lacerda AE, Pereverzev A, Klockner U, Schneider T & Perez-Reyes E (1999*a*). Cloning and expression of a novel member of the low voltage-activated T-type calcium channel family. *J Neurosci* **19**, 1912–1921.

Lee JH, Gomora JC, Cribbs LL & Perez-Reyes E (1999*b*). Nickel block of three cloned T-type calcium channels: low concentrations selectively block α1H. *Biophys J* **77**, 3034–3042.

Lee SE, Ahn DS & Lee YH (2009). Role of T-type Ca channels in the spontaneous phasic contraction of pregnant rat uterine smooth muscle. *Korean J Physiol Pharmacol* **13**, 241–249.

Liu Y, Zeng W, Delmar M & Jalife J (1993). Ionic mechanisms of electronic inhibition and concealed conduction in rabbit atrioventricular nodal myocytes. *Circulation* **88**, 1634–1646.

Majeed IA, Murray WJ, Newton DW, Othman S & Al-Turk WA (1987). Spectrophotometric study of the photodecomposition kinetics of nifedipine. *J Pharm Pharmacol* **39**, 1044–1046.

Martin RL, Lee JH, Cribbs LL, Perez-Reyes E & Hanck DA (2000). Mibefradil block of cloned T-type calcium channels. *J Pharmacol Exp Ther* **295**, 302–308.

McDonough SI & Bean BP (1998). Mibefradil inhibition of T-type calcium channels in cerebellar purkinje neurons. *Mol Pharmacol* **54**, 1080–1087.

McHale NG & Allen JM (1983). The effect of external Ca^{2+} concentration on the contractility of bovine mesenteric lymphatics. *Microvasc Res* **26**, 182–192.

McHale NG, Allen JM & Iggulden HL (1987). Mechanism of alpha-adrenergic excitation in bovine lymphatic smooth muscle. *Am J Physiol* **252**, H873–878.

McHale NG & Roddie IC (1976). The effect of transmural pressure on pumping activity in isolated bovine lymphatic vessels. *J Physiol* **261**, 255–269.

Mikami A, Imoto K, Tanabe T, Niidome T, Mori Y, Takeshima H, Narumiya S & Numa S (1989). Primary structure and functional expression of the cardiac dihydropyridine-sensitive calcium channel. *Nature* **340**, 230–233.

Moosmang S, Haider N, Bruderl B, Welling A & Hofmann F (2006). Antihypertensive effects of the putative T-type calcium channel antagonist mibefradil are mediated by the L-type calcium channel Cav1.2. *Circ Res* **98**, 105–110.

Moosmang S, Schulla V, Welling A, Feil R, Feil S, Wegener JW, Hofmann F & Klugbauer N (2003). Dominant role of smooth muscle L-type calcium channel Cav1.2 for blood pressure regulation. *EMBO J* **22**, 6027–6034.

Muthuchamy M, Gashev A, Boswell N, Dawson N & Zawieja D (2003). Molecular and functional analyses of the contractile apparatus in lymphatic muscle. *FASEB J* **17**, 920–922.

Nelson MT, Patlak JB, Worley JF & Standen NB (1990). Calcium channels, potassium channels, and voltage dependence of arterial smooth muscle tone. *Am J Physiol* **259**, C3–18.

Ono K & Iijima T (2005). Pathophysiological significance of T-type Ca^{2+} channels: properties and functional roles of T-type Ca^{2+} channels in cardiac pacemaking. *J Pharmacol Sci* **99**, 197–204.

Pignier C & Potreau D (2000). Characterization of nifedipine-resistant calcium current in neonatal rat ventricular cardiomyocytes. *Am J Physiol Heart Circ Physiol* **279**, H2259–2268.

Seino S, Chen L, Seino M, Blondel O, Takeda J, Johnson JH & Bell GI (1992). Cloning of the α_1 subunit of a voltage-dependent calcium channel expressed in pancreatic β cells. *Proc Natl Acad Sci U S A* **89**, 584–588.

Snutch TP, Sutton KG & Zamponi GW (2001). Voltage-dependent calcium channels – beyond dihydropyridine antagonists. *Curr Opin Pharmacol* **1**, 11–16.

Sui GP, Wu C & Fry CH (2001). Inward calcium currents in cultured and freshly isolated detrusor muscle cells: evidence of a T-type calcium current. *J Urol* **165**, 621–626.

Tanabe T, Takeshima H, Mikami A, Flockerzi V, Takahashi H, Kangawa K, Kojima M, Matsuo H, Hirose T & Numa S (1987). Primary structure of the receptor for calcium channel blockers from skeletal muscle. *Nature* **328**, 313–318.

van Helden DF (1993). Pacemaker potentials in lymphatic smooth muscle of the guinea-pig mesentery. *J Physiol* **471**, 465–479.

van Helden DF, von der Weid PY & Crowe MJ (1995). Electrophysiology of lymphatic smooth muscle. In *Interstitium, Connective Tissue, and Lymphatics*, eds. Bert J, Laine GA, McHale NG, Reed R & Winlove P. pp. 221–236. Portland Press, London.

von der Weid P-Y, Crowe MJ & van Helden DF (1996). Endothelium-dependent modulation of pacemaking in lymphatic vessels of the guinea-pig mesentery. *J Physiol* **493**, 563–575.

von der Weid PY, Lee S, Imtiaz MS, Zawieja DC & Davis MJ (2014). Electrophysiological properties of rat mesenteric lymphatic vessels and their regulation by stretch. *Lymphat Res Biol* **12**, 66–75.

von der Weid PY, Rahman M, Imtiaz MS & van Helden DF (2008). Spontaneous transient depolarizations in lymphatic vessels of the guinea pig mesentery: pharmacology and implication for spontaneous contractility. *Am J Physiol Heart Circ Physiol* **295**, H1989–2000.

Welsh DG, Morielli AD, Nelson MT & Brayden JE (2002). Transient receptor potential channels regulate myogenic tone of resistance arteries. *Circ Res* **90**, 248–250.

Welsh DG, Nelson MT, Eckman DM & Brayden JE (2000). Swelling-activated cation channels mediate depolarization of rat cerebrovascular smooth muscle by hyposmolarity and intravascular pressure. *J Physiol* **527**, 139–148.

Xu WX, Kim SJ, Kim SJ, So I, Kang TM, Rhee JC & Kim KW (1996). Effect of stretch on calcium channel currents recorded from the antral circular myocytes of guinea-pig stomach. *Pflugers Arch* **432**, 159–164.

Yanai Y, Hashitani H, Kubota Y, Sasaki S, Kohri K & Suzuki H (2006). The role of Ni^{2+}-sensitive T-type Ca^{2+} channels in the regulation of spontaneous excitation in detrusor smooth muscles of the guinea-pig bladder. *BJU Int* **97**, 182–189.

Young RC, Smith LH & McLaren MD (1993). T-type and L-type calcium currents in freshly dispersed human uterine smooth muscle cells. *Am J Obstet Gynecol* **169**, 785–792.

Zawieja DC (2009). Contractile physiology of lymphatics. *Lymphat Res Biol* **7**, 87–96.

Zhang R, Gashev AA, Zawieja DC, Lane MM & Davis MJ (2007). Length-dependence of lymphatic phasic contractile activity under isometric and isobaric conditions. *Microcirculation* **14**, 613–625.

Zhou Z & Lipsius SL (1994). T-type calcium current in latent pacemaker cells isolated from cat right atrium. *J Mol Cell Cardiol* **26**, 1211–1219.

Additional information

Competing interests

None declared.

Author contributions

All experiments were undertaken at the University of Calgary. S.L. carried out most of the experiments and the data analysis; he was helped by S.R. for the confocal imaging experiments and by P.-Y.v.d.W. for the electrophysiology experiments. P.-Y.v.d.W. and S.L. conceived and designed the project. All authors wrote and critically reviewed the manuscript and gave final approval of the version to be published.

Funding

We would like to acknowledge the support of the Live Cell Imaging Facility of the University of Calgary's Snyder Institute for Chronic Diseases, which is funded by an equipment and infrastructure grant from the Canadian Foundation for Innovation (CFI) and the Alberta Science and Research Authority. This study was supported by grants from the National Institute of Health (NIH HL096552) and the Canadian Institutes of Health Research.

Acknowledgements

None declared.